Dosimetry for gadolinium neutron capture therapy (GdNCT)☆

Shirin A. Enger[a], Valerio Giusti[b], Marc-André Fortin[c], Hans Lundqvist[a], Per Munck af Rosenschöld[d]

[a]*Department of Radiology, Oncology and Radiation science, Uppsala University Hospital, 751 85 Uppsala, Sweden*
[b]*Dept. of Civil and Industrial Engineering, University of Pisa, Via Diotisalvi 2, 56126 Pisa, Italy*
[c]*Axe métabolisme, santé vasculaire et rénale, Centre hospitalier universitaire de Québec (AMSVR-CHUQ), Centre de recherche sur les matériaux avancés (CERMA) and Department of Engineering Materials, Université Laval, Québec G1V 0A6, Canada*
[d]*Radiation Physics, Lund University Hospital, SE-22185 Lund, Sweden*

Abstract

Background: Gadolinium (Gd) neutron capture therapy (GdNCT) is based on a neutron capture reaction (NCR) that involves emission of both short and long range products. The aim of this study was to investigate both the microscopic and macroscopic contributions of the absorbed dose involved in GdNCT.
Methods: Cylindrical containers with diameters 1-30 mm filled with a solution of Gd were irradiated with epithermal neutrons. The background neutron dose as well as the prompt gamma dose has been calculated and measured by means of film dosimetry for the largest cylinder. Monte Carlo codes MCNP5(b) and GEANT4 have been utilized for calculation the absorbed dose.
Results and discussion: Results from the film dosimetry are in agreement with the calculations for high doses while for low doses the measured values are higher than the calculated results. For the largest cylinder, the prompt gamma dose from GdNCT neutron is at least five times higher than the background dose. For a cell cluster model, in the first 0.1 mm the major contribution to the absorbed dose is from IC electrons. If Gd atoms were homogeneously distributed in the nuclei of all tumour cells, capture events between neutron and Gd atoms close to DNA could kill the tumour cells and give cross-fire dose from IC electrons to the cells located in the 0.1 mm range.
Conclusions: For a correct GdNCT dosimetry both microscopic part of the dose delivered by short-range low energy electrons and macroscopic part delivered by the prompt gamma should be considered

Keywords: Gadolinium neutron capture therapy, Tumour therapy, Gadolinium nanoparticle

1. Introduction

Neutron Capture Therapy (NCT) is a radiotherapeutic approach that has been under development for decades (Locher, 1936). In NCT the patient is administered with a neutron capture agent that accumulates significantly in the target while the concentration in the blood and healthy tissue are kept at lower levels during the time of the procedure. The target area is then irradiated with neutrons, that reacting with the capture agent can give an adequate absorbed dose to the target while keeping the damage to healthy tissue at an acceptable level. NCT requires a high level of the different technological components involved, since the physical parameters interact in a rather complex way. The interaction with the nuclei of the biological tissues (mainly absorption by hydrogen) strongly attenuates the thermal neutrons (energy up to 0.4 eV) thus preventing their direct use to irradiate deeply sited target volumes. Epithermal neutrons (energy range 0.4 eV−10 keV) are considered instead to be optimal for NCT since they are slowed down

☆This is the Postprint version of an Accepted Manuscript published by Elsevier in Radiation Measurements. The interested reader is kindly asked to read the original publication available at the following link: http://dx.doi.org/10.1016/j.radmeas.2013.05.009.

by scattering collisions (primarily with hydrogen nuclei) and generate a thermal neutron distribution with a peak at some depth in the tissue (Capala et al., 2003; Chadha et al., 1998), thus enabling the delivery of a sufficiently high and pure thermal neutron flux to the target volume. Neutron sources currently available for NCT are provided by nuclear reactor and large accelerator-based neutron beams. However, these facilities are often placed far from major hospitals and their use in clinical trials may arise some practical problems. Ongoing research regarding the development of small accelerator-based NCT, suitable to accommodate within hospitals and health research centres, will hopefully facilitate a future wide-spread clinical use of this technology. (Barth et al., 2012; Blue and Yanch, 2003; Harling and Riley, 2003). Only a limited number of nuclides have the potential to be truly efficient in NCT (Carlsson et al., 2002). Most studied is ^{10}B due to its relatively high thermal neutron cross section (3800 b). The range in tissue of the two high Linear Energy Transfer (LET) reaction products, an energetic α particle and ^{7}Li nucleus, 7.3 and 4.0 μm respectively, is of the same order of magnitude of the cell dimensions. The high energy of these products makes them efficient in killing cells surrounding the point where the reaction took place (Coderre and Morris,1999). In 94% of the cases, a photon with energy of 475 keV is also emitted (Barth et al. 2012; Goldenberg et al., 1984; Hawthorne, 1993; Hosmane et al., 2012; Hosmane, 2011; Kueffer et al., 2013; Shelly et al., 1992, Sweet, 1997). Gadolinium (Gd) is another promising candidate in the process of elaborating compounds for NCT (De Stasio et al., 2005; De Stasio et al., 2001; Enger et al., 2006a,b; Tokumitsu et al., 1999; Gierga et al., 2000; Goorley et al., 2002; Goorley and Nikjoo, 2002; Hosmane, 2011; Jono et al., 1999; Martin et al., 1988; Masiakowski et al., 1992; Salt et al., 2004; Shih and Brugger, 1992a,b; Stepanek, 2003; Takagaki and Hosmane, 2007; Tokuuye et al., 2000). Thermal neutron cross section of naturally occurring Gd (49000 b) is dominated by ^{157}Gd (254000 b), which is 60 times larger than that of ^{10}B. Another interesting characteristic of Gd is that it is also used as a contrast enhancer in more than 30% of all clinical magnetic resonance imaging (MRI) investigations, in the form of intravenously injected Gd chelates. MRI could be performed before the neutron irradiation for therapy that might allow an assessment of the Gd concentration in the tissue to be used in the treatment planning phase (Hoffmann et al., 1999), akin to what has been proposed for positron emission tomography-based planning in BNCT. In Gd neutron capture therapy (GdNCT), the selective therapeutic effect can be achieved by targeting sufficient amounts of ^{157}Gd nuclide to the target tumour cells. GdNCT procedures have been hindered by poor cell retention of traditional Gd-containing MRI contrast agents (mostly monochelated Gd compounds) (De Stasio et al., 2005; De Stasio et al., 2001). In order to achieve higher Gd uptakes not only in tumours but also into healthy cells, a variety of biocompatible macromolecular and nanoparticulate assemblies have been designed. Recently, higher tumour regression rates have been achieved using tumour-targeted Gd delivery systems. Compounds such as chitosan-loaded with Gd-DTPA (426 nm diameter, 9.3% Gd) can enter the tumour cells through endocytosis and significantly enhance Gd uptake and retention, by a factor of 200 compared with Gd monochelates (Shikata et al., 2002). Chitosan-Gd-DTPA coupled with GdNCT procedures proved efficient to suppress tumour growth in small animals (Tokumitsu et al., 2000). Gd-containing lipid nanoemulsions (Watanabe et al., 2002) and liposomes (Le and Cui, 2006a) have also been developed, offering Gd-containing units of smaller size that could prolong the blood circulation time of Gd and therefore more easily penetrate the tumour tissues (Le and Cui, 2006b). Nanoparticles and macromolecular compounds can also be conjugated with targeting agents such as folate ligands that bind to the surface of certain cancer cells, thus achieving even higher targeting yields and considerably enhancing the retention of Gd to the target tissues prior to NCT (Oyewumi and Mumper, 2003). In vivo, the large size of these constructs may be a limitation to efficient extravasation from capillaries. Recent advances in the field of contrast agents for MRI have focused on the development of nanometric molecular constructs based on assemblies of polymers with inorganic cores containing Gd. Some compounds can be as small as 2−3 nm in diameter and can contain between 100 and 1000 atoms of Gd (Fortin et al., 2007). The neutron capture reaction of ^{157}Gd is however very different from that of 10 B. The nature and energy of the emitted radiation during the ^{157}Gd and ^{10}B neutron capture reactions necessarily have a strong incidence on the efficacy of the therapy. The capture of neutrons by ^{157}Gd provokes a sequence of complex decay transitions that generate low-LET prompt gammas with energies ranging from 0.08 to 7.8 MeV. These gammas are accompanied by the emission of internal conversion (IC) electrons ranging in energy from 79 keV to 6.9 MeV (Stepanek, 2003) IC electrons leave orbital electron vacancies that de-excite by emitting X-rays or low energy Auger electrons. Simulations have been performed in the ^{157}Gd neutron capture reaction, and indicated a yield of 5.0 Auger electrons, 1.8 γ-photons, 0.69 IC electrons, 0.84 X-ray photons, 5.5 free-bound X-rays and 1.0 recoil nucleus. The success of GdNCT is determined by the relative biological effectiveness (RBE) of the radiation products, by the accumulation of sufficient concentrations of Gd in the tumour cells as well as by the properties and characteristics of the beam. The RBE for Auger electrons is dependent on the location of their emission with respect

Table 1: Stable gadolinium isotopes.

	^{152}Gd	^{154}Gd	^{155}Gd	^{156}Gd	^{157}Gd	^{158}Gd	^{160}Gd
Natural abundance (%)	0.20	2.18	14.80	20.47	15.65	24.84	21.86
Thermal neutron cross section (barns)	700	60	61000	2	255000	2.41	1

to the DNA and may be greater than one if the Gd atoms are attached to the DNA. The nanometer range of the Auger electrons causes a high-linear energy transfer (LET) which produces a biological damage directly through ionization as well as indirectly through the production of free radicals in the DNA (Salt et al., 2004; Stepanek, 2003). In order to benefit of the RBE characteristic of the short-range Auger electrons, GdNCT has to be performed making use of Gd carrying compounds which can 1) be efficiently internalized into cells, and 2) migrate as close as possible to the cell nucleus. According to previous studies, the poor cell internalization rates of commercial Gd chelates (such as Gd-DTPA), are not appropriate as an efficient GdNCT agent since these compounds are mainly kept outside the cell and cannot produce enough Auger electron-induced DNA damages (Franken et al., 2006; Martin et al., 1989, 1988). However, for in-vitro cell experiments, the prompt gammas would escape the medium without substantially contributing to the absorbed dose. In an in-vivo situation, these prompt gammas would deposit their energy in the surrounding tissue and dominate over the absorbed dose from IC and Auger electrons. Due to the long path length of the prompt gammas, delivery of the dose to the surrounding tissue occurs even if there is no Gd present in the normal tissue thus reducing the local effect of GdNCT. The complexity of the emission spectra of Gd neutron capture reaction requires careful investigations both in-vitro and in-vivo prior to the establishment of clinical procedures. The evaluation of the therapeutic dose delivered microscopically (to nearby cells) by short-range low energy electrons and macroscopically by long- range gamma rays, at given distances from the radiation emission site, is an aspect that is at the very core of GdNCT research. Therefore, the aim of the present work is to investigate all the components of the absorbed dose involved in GdNCT.

2. Materials and Methods

2.1. Measurement of photon absorbed dose

A cylindrical container (radius 1.5 cm, height 3 cm) was filled with the Gd MRI contrast agent OMNISCAN^{TM}(0.5 mmol/ml, 78625 ppm), consisting of stable Gd isotopes with the natural abundances as shown in Table 1, diluted with water (1:39) to give a concentration of about 2000 ppm of Gd (2 mg Gd/mL). The container was placed inside a 20x20x15 cm^3 PMMA phantom with its axis at a depth of 4.5 cm and then irradiated with epithermal neutrons (Matsumoto, 1991) at the Studsvik BNCT facility (Sweden) (Giusti et al., 2003; Munck af Rosenschold et al., 2003). The absorbed dose was measured; the setup is illustrated in Fig. 1, using a film that is chemically altered by the radiation, resulting in a measurable shift in colour (GAFChromic^{TM}) (Butson et al., 2002).

The film has been calibrated by irradiating 2x2 cm^2 pieces of it in a ^{137}Cs photon field (Gammacell 40 Exactor) producing a known dose rate of 1.30 Gy/min. A PMMA slice was placed around the film to obtain an adequate build-up zone. The error of the absorbed dose was estimated to ±0.05 Gy. The calibration films, as well as the films from the Gd-measurements, were scanned by a transmission scanner (DUOSCAN f40, AGFA) to monitor the dose-induced density changes. For the calibration films the absorbed dose was plotted against the optical density to create a calibration curve that was used to evaluate the films irradiated in the PMMA phantom with epithermal neutrons. The digital optical density distribution from the film measurements were analysed using MATLAB. Data were smoothed and compressed by a technique known as adaptive Gaussian low pass filtering and sub sampling (Gonzalez and Woods, 2002).

2.2. Monte Carlo calculations

Measurements were compared with Monte Carlo (MC) calculations to verify the accuracy of the latter. The MC calculations were performed with two different codes: MCNP version (X-5 Monte Carlo Team, 2003) and Geant4 version 9.2 patch 2 (Agostinelli et al., 2003; Carrier et al., 2004; Poon and Verhaegen, 2005). Both codes can handle multiple materials in complex geometries and have three-dimensional capabilities coupled with advanced radiation

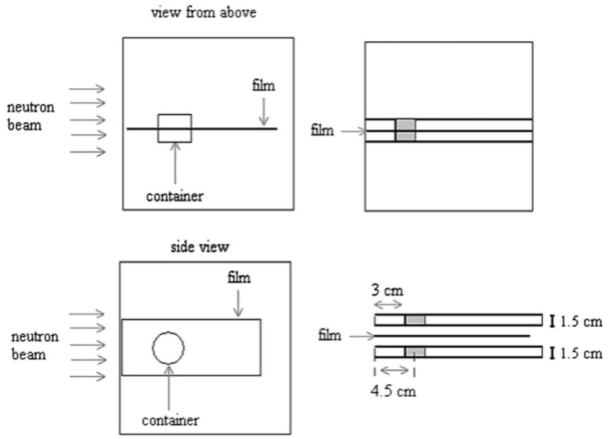

Figure 1: A Gd-container with a diameter of 3 cm was placed with its axis at 4.5 cm depth (x-axis), inside a 20x20x15 cm^3 phantom. The container consisted of two identical parts (diameter 3 cm, height 1.5 cm) and the film was positioned in between of the two parts. Irradiations were performed with the container filled with the Gd solution (2000 ppm) as well as with water only.

transport physics and cross section libraries. However, physics is implemented in different ways in the two codes. In the evaluations of Kerma and absorbed dose from both the Gd neutron capture reaction and the background radiation, MCNP was used since it is the most accurate and commonly used code for low energy neutron transport calculations and is very well investigated (Enger et al., 2006a,b). For technical reasons, the MC model of the Studsvik BNCT facility was divided into three regions as it is shown is Fig. 2 (Giusti et al., 2003; Munck af Rosenschold et al., 2003). The simulations performed in this work considered only the last region of the model, i.e. a trapezoidal collimator ending with an aperture of 14x10 cm^2 and a 8 mm thick ^{6}Li filter used to cut completely down the thermal neutron component of the beam. The neutron and photon sources for this region of the geometry were represented by the respective spectra obtained by previous MCNP simulations at the end of the region II. The Kerma and absorbed dose distributions were calculated in 100 slices, each one of them 1 mm thick both in the beam direction (x-axis) and the direction perpendicular to the beam (y-axis) while 1 cm thick in the vertical direction (z-axis). The Kerma and absorbed dose were normalized to 1 for the highest value. Three additional Gd-containers of 1, 5 and 15 mm diameter, 3 cm height and with 2000 ppm Gd concentration were also considered for the simulations. In each of these cases, the axis of the cylinder was placed at a depth of 4.5 cm.

Contribution of short-range radiation to the delivered dose at the sub-cellular level. In order to evaluate the crucial contribution of short-range radiation phenomena to the overall dose to the cells, the spectrum of ^{158}Gd per (n,γ) reaction of ^{157}Gd was studied in more detail. A spherical cell model with a diameter set to 12 μm and with a spherical nucleus of 3 μm diameter, centred in the cell, was considered for this study. The absorbed dose contributions from IC-photons, IC-electrons, fluorescence, Auger electrons were calculated according to this model. Three different theoretical Gd distributions were considered and the generated absorbed dose was calculated accordingly: (a) Gd internalized only in the cell nucleus, (b) Gd only in the plasma and (c) Gd homogeneously distributed in the cell (Fig. 3). We considered a cell model surrounded by a spherical water phantom (20 cm in diameter). Contributions to the absorbed dose from different radiation products were calculated in the surrounding water sphere for the case (c), i.e. when Gd is homogeneously distributed in the cell. The emission spectra of ^{158}Gd were taken from Stepanek (Stepanek, 2003). The calculations for this part of the study were performed with the MC code Geant4.

3. Results

The 30 mm diameter cylindrical container, filled with a solution with 2000 ppm of Gd, was placed in a PMMA phantom and irradiated with epithermal neutrons at the Studsvik BNCT facility. Fig. 4 shows the film after the neutron irradiation both in the case with the container filled with water only (left) and with the container filled with 2000 ppm

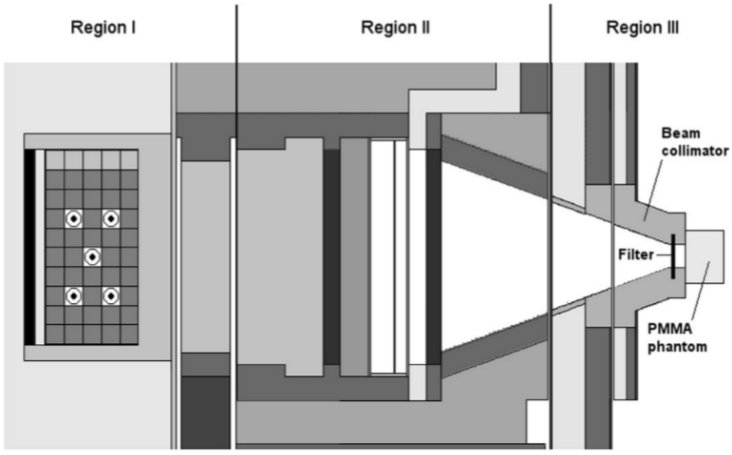

Figure 2: Horizontal section of the MCNP model for the beam filter and beam collimators at Studsvik. Region I includes the reactor core, a 20 cm thick Al layer and the Cd shield. Region II starts after the Cd shield and extends to the end of the first Pb collimator section. The reported simulations considered only the region III, which includes the last part of the beam line, i.e. a collimator delimiting a 14x10 cm^2 field and 8 mm thick ^{6}Li filter. A 20x20x15 cm^3 PMMA phantom is placed in front of the beam port. The calculated neutron spectrum used as an input source in the present work has been validated previously by activation and ionisation chamber measurements (Giusti et al., 2003; Munck af Rosenschold et al., 2003).

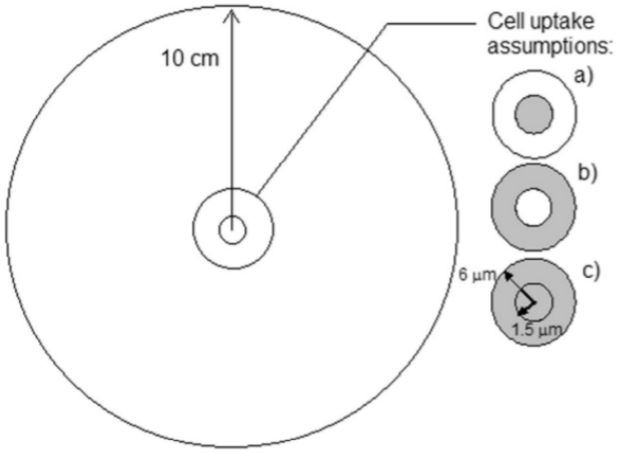

Figure 3: The absorbed dose per decay from IC-photon, IC-electron, fluorescence, Auger electrons was calculated for a spherical cell model. The diameter of the cell nucleus is 3 μm while the diameter of the cell is 12 μm. Three different scenarios were studied: i.e. when the (n,γ) reaction of ^{157}Gd occurs (a) only in cell nucleus, (b) only in cell plasma or (c) in the whole cell. The cell model is surrounded by a spherical water phantom, 20 cm diameter. The absorbed dose in the surrounding water sphere has been calculated for the last scenario, i.e. when Gd is homogeneously distributed in the cell.

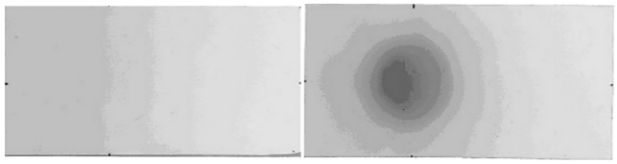

Figure 4: Film after neutron irradiation with the 30 mm cylindrical container filled with water only (left) and with 2000 ppm Gd solution (right).

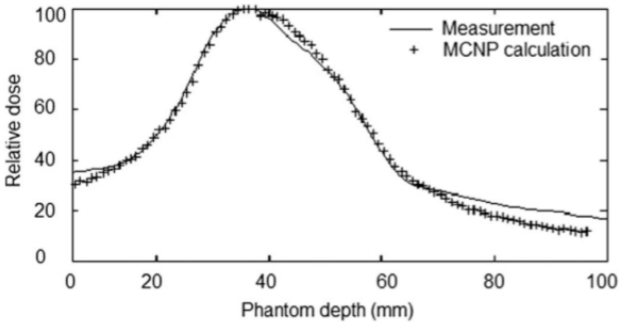

Figure 5: Measured and calculated absorbed dose in percentage of their maximum value plotted as a function of the phantom depth.

Gd solution (right). Fig. 5 shows the comparison of the measured and calculated absorbed doses (both normalized to their maximum value) as a function of the phantom depth.

MCNP calculated Kerma and photon absorbed dose (Gy/h) as a function of phantom depth (cm) are presented in Fig. 6 for all the Gd container diameters considered. The estimated uncertainties of the calculations (not shown in the graph) were in the range of 1−3% (1SD). The absorbed dose calculations were made both with and without Gd in the container for the largest diameter.

The thermal neutron fluence rate depression due to the presence of Gd is shown in Fig. 7a as a function of phantom depth and the Gd container diameters. Fig. 7b shows the fast neutron fluence rate for the same diameters of the cylinder.

Table 2 shows the calculated absorbed dose in the cell nucleus and cell plasma if (a) Gd is internalized only in the cell nucleus, (b) Gd is only in the plasma and (c) if Gd is homogeneously distributed in the cell.

Fig. 8 illustrates the absorbed dose per decay in the surrounding spherical water phantom for different radiation products.

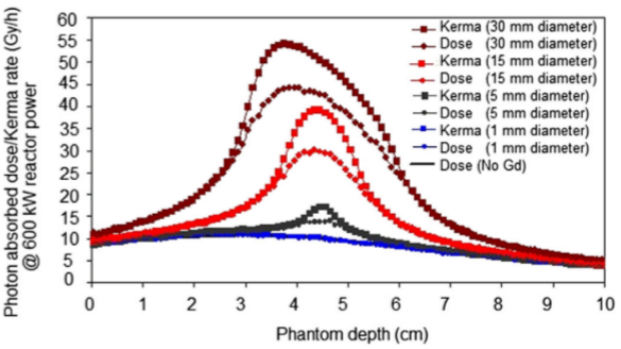

Figure 6: MCNP calculated photon absorbed dose and Kerma rate (Gy/hr) as a function of the phantom depth (cm). The simulations were performed with Gd for different container diameters: 1, 5, 15 and 30 mm. The axis of all the containers has been placed at a depth in the phantom of 4.5 cm. For the largest container a simulation with no Gd in the container has also been performed.

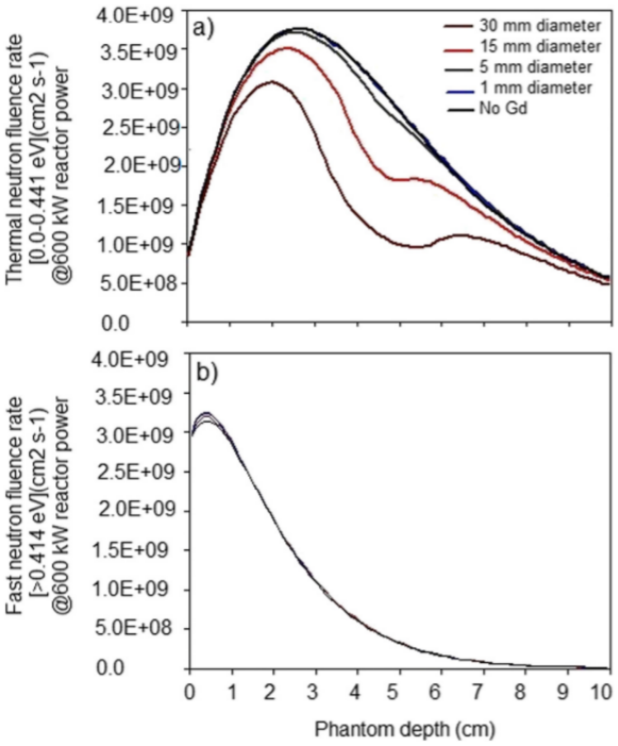

Figure 7: a. Thermal neutron fluence rate as a function of phantom depth for different cylinder diameters 1, 5, 15 and 30 mm with Gd. For the largest cylinder a simulation without Gd has also been performed. b shows the fast neutron fluence rate for the same upset.

Table 2: Calculated absorbed dose in the cell nucleus and cell plasma from IC and Auger electrons if the (n,γ) reaction of ^{157}Gd occurs in the nucleus, the cell plasma or the whole cell.

Gd internalized inside	Absorbed dose in nucleus (Gy/decay)			Absorbed dose in plasma (Gy/decay)		
	IC electron	Auger electrons	Total nucleus	IC electron	Auger electrons	Total plasma
Nucleus	5.63E-3	3.24E-3	8.88E-3	4.20E-4	4.15E-7	4.21E-4
Cytoplasma	4.04E-4	4.18E-7	4.04E-4	3.78E-4	5.18E-5	4.30E-4
Cell	4.92E-4	5.08E-5	5.42E-4	3.78E-4	5.10E-5	4.29E-4

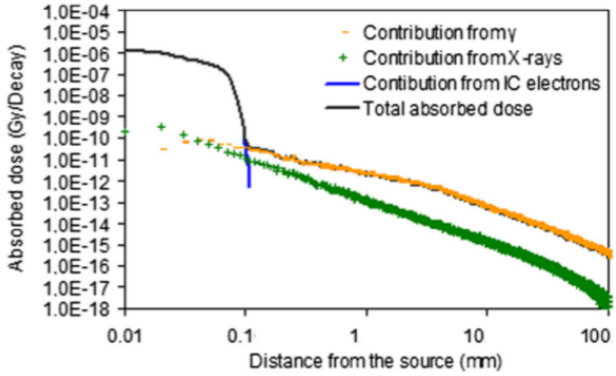

Figure 8: Contribution to the absorbed dose from different radiation products in the surrounding water sphere when Gd is homogeneously distributed in the cell.

4. Discussion

Neutron capture therapy is, in theory, an attractive therapeutical modality. The first experimental set-up during the fifties used fairly pure thermal neutrons that had a too low tissue penetration, producing as a consequence a too high skin doses (Sweet, 1997). Today, in most cases, neutron sources for NCT deliver epithermal neutrons that, being moderated by the soft tissue, produce a peak of thermal neutron at some depth thus providing a skin-sparing dose distribution. The technology of reactor-based neutron fields for NCT has probably reached a level so high that it is quite difficult to improve it. Some technical progresses may still be possible using accelerator-produced neutrons but the main advantage here is probably that this technique will allow hospital-based therapy with a rotational gantry arrangement.

The major problem has been to deliver the NCT agent specifically to the target area. So far the main application has been boron neutron capture therapy (BNCT). To be successful as mono-therapy this therapy needs $10^8 - 10^9$ boron atoms delivered to every single tumour cell and at least a tenfold fewer to the surrounding healthy cells (Hartman and Carlsson, 1994). After neutron absorption, ^{10}B splits into an energetic alpha particle and lithium nucleus. The short range and high energy of these products make them efficient at killing the cell or neighbouring cell in which the neutron capture took place.

In GdNCT, the neutron capture reaction includes both very short range (nm) and long range (mm to cm) products. The efficiency of GdNCT is anticipated to be driven by the proximity of Gd to DNA, and also by the overall concentration of Gd in the tissue (to benefit from cross-fire radiation effects).

In the first part of the present work, prompt gamma absorbed dose from Gd neutron capture reaction was measured and calculated. To verify the accuracy of the MC calculations a PMMA phantom embedding a cylindrical container filled with a Gd solution (2000 ppm of Gd, natural isotopic composition) was irradiated with epithermal neutrons and the absorbed dose was measured with a radiochromic film. The IC and Auger electrons were not considered in the calculations of this part of the study. The Gd neutron capture reaction emits low-LET gamma rays and characteristic X-rays with an average energy of ~2.2 MeV and a path length of several centimeters. The measured prompt gamma absorbed dose, normalized to the maximum value, is compared to the MCNP calculated dose in Fig. 5. For high doses, the measurement results agree well with the calculated values while for low doses the measured values are higher than the calculated results. As expected, both the calculated and measured prompt gamma dose show a maximum close to 3 cm depth, since the incident epithermal neutron beam produces a thermal neutron fluence peak around that depth in the phantom. The difference between the prompt gamma dose and background dose decreases with the distance from the Gd container. The background dose is that induced by neutron capture reactions with all the present nuclides except Gd. Thermal neutrons cause nuclear reactions in normal tissue mainly through ^{14}N(n,p)^{14}C and ^{1}H(n,γ)^{2}H. Although the cross sections of these reactions are small compared to that of Gd, the concentration of H and N atoms is considerably higher than that of Gd inside the cylindrical container.

In Fig. 6, the calculated Kerma rate and prompt gamma absorbed doses (Gy/h) with Gd in containers of different diameters are presented as a function of phantom depth (cm). All the cylindrical Gd containers had a concentration of 2000 ppm of Gd (natural isotopic composition). For the largest container a simulation without Gd was also performed. The Kerma and prompt gamma absorbed dose is higher in large tumours than the absorbed dose in small tumours. On the other hand the cross-fire dose from larger tumours to normal tissue is also higher. For the largest tumour (30 mm in diameter) the prompt gamma absorbed dose from Gd neutron capture reaction is at least 5 times higher than the background dose. The absorbed dose is high inside the tumour and decreases fast with the distance from the tumour due to the inverse square factor. The dose drops twofold within 1 cm from the edge of the tumour and fall to the background level after 3 cm. The absorbed dose in the case of the smallest Gd container considered (1 mm diameter and 3 cm high, dimensions that resemble those of a brachytherapy needle) is at the same level of the background dose. This was expected since the surface area of the container affects the distribution of the absorbed dose (Shih and Brugger, 1992a,b): Gd containers with larger surface deliver higher dose.

Fig. 7a and b illustrates the thermal neutron fluence rate and fast neutron fluence rate distribution as a function of the phantom depth and the Gd container size for a constant Gd concentration (2000 ppm). As the volume of the container increases, the thermal neutron fluence rates across the volume decreases. The non- uniformity of the thermal neutron fluence rate is significant for the largest tumour here considered (i.e. 3 cm diameter). Because of this non-uniformity of the neutron fluence, the normal tissue in front of the tumour receives a higher photon absorbed dose than the normal tissue behind the tumour. Previous studies had also shown that the relationship between Gd concentration

and photon dose is not linear, because of the thermal neutron flux depression (Munck af Rosenschold et al., 2002). Fast neutron fluence rate on the other hand is the same for all the container sizes as expected and does not change with the Gd container size.

Due to the large neutron absorption cross section of Gd there is a significant depression of the thermal neutron fluence even with small amounts of Gd in the normal tissue. The thermal neutron fluence and the capture reaction rates will decrease with depth giving rise to a non-homogeneous absorbed dose distribution in the tumour area and increasing the dose to normal tissue. Recently, progresses in nanoparticle enhanced MRI has led to development of ultra-small Gd_2O_3 nanocrystals (Fortin et al., 2007) that could be more efficiently delivered to tumour cells than larger size lipid emulsions, vesicles and macromolecular constructs already tested in-vivo. The very small size and the optimal Gd packing density of Gd oxide allows the labelling of matching size targeting molecules and the possibility to more effectively deliver contrast agents to targeted areas in the body. Such targeting techniques could increase the concentration of Gd in tumour and decrease it in the normal tissue preventing the thermal neutron flux depression at the target and also decreasing the absorbed dose to healthy tissue.

It has been observed that the Auger effect in the Gd capture reaction improves the radiation efficacy (Shih and Brugger, 1992a,b) if Gd is accumulated close to the DNA molecule. In the second part of the paper the spectrum of ^{158}Gd per (n,γ) reaction of ^{157}Gd was studied in detail. The absorbed dose contribution from IC-photon, IC-electron, fluorescence, Auger electrons was calculated for a spherical cell model. Table 2 shows the calculated absorbed dose in the cell nucleus and cell plasma if the (n,γ) reaction of ^{157}Gd occurs in the nucleus, cell plasma or in the cell (both nucleus and plasma). The recoil nucleus with an average energy of 2 eV and free bound X-rays with an average energy of 20 eV do not contribute to the absorbed dose as these energies are too low to ionize the water molecules and will only contribute to the heating. As expected, the cell nucleus receives the highest absorbed dose when (n,γ) reaction of ^{157}Gd occurs in the nucleus. Auger electrons deposit all their energy locally and may produce double strand brakes if Gd atom is attached to the DNA. Fig. 8 illustrates the absorbed dose in the surrounding water phantom when Gd atoms are homogeneously distributed in the cell (scenario c of Fig. 3). In the first 0.1 mm (16 times the cell radius for a 6 μm radius cell) the major contribution to the absorbed dose is from IC electrons. At larger distances, the contribution from prompt gamma increases and dominates the absorbed dose even if the absolute value is some 4 order of magnitude lower than the maximum. If Gd atoms are homogeneously distributed in the nuclei of all tumour cells, capture event between neutron and Gd atoms close to DNA could kill the tumour cells and give cross-fire dose from IC electron to the cells located in the 0.1 mm range (about 7−8 compact layers of cells would be affected around each Gd-containing cell). The neighbouring tumour cells will also get cross-fire dose from prompt gammas. The major drawback is that normal tissue several cm from the capture site still receives absorbed dose from gamma radiation. Most of the prompt gamma energy will leave the treatment volume and deposit the energy in the normal tissue. For IC and Auger electrons the emitted energy will be deposited in the tumour area and will enhance the absorbed dose significantly.

5. Conclusion

For a correct GdNCT dosimetry both the microscopic part of the dose delivered by short-range low energy electrons and the macroscopic part delivered by the prompt gamma should be considered. The results from our study highlight the importance of concentrating the Gd compounds as close as possible into the cell nucleus, in order to benefit from the contribution of IC electrons, Auger electrons. New GdNCT compounds using both cell and nucleus internalization strategies (double-step targeting) could have a much larger radio-therapeutic effect on tumour cells. The very small size and optimal Gd packing density of the compounds allows the labelling of matching size targeting molecules and the possibility to more effectively deliver contrast agents to targeted areas in the body. Such targeting techniques could increase the concentration of Gd in tumours and decrease it in the normal tissue preventing the thermal neutron flux depression at the target and also decreasing the absorbed dose to healthy tissue.

Conflict of interest

There are no conflicts of interest for any of the authors requiring disclosure for this project.

Acknowledgements

The authors would like to thank Studsvik Medical AB.

References

Agostinelli, S., et al., 2003. Geant4 - a simulation toolkit. Nucl. Instruments Methods Phys. Res. A 506, 250−303.

Barth, R.F., Vicente, M.G.H., Harling, O.K., Kiger, W.S., Riley, K.J., Binns, P.J., 2012. Current status of boron neutron capture therapy of high grade gliomas and recurrent head and neck cancer. Radiat. Oncol. 7, 146−167.

Blue, T.E., Yanch, J.C., 2003. Accelerator-based epithermal neutron sources for boron neutron capture therapy of brain tumors. J. Neurooncol. 62, 19−31.

Butson, M.J., Cheung, T., Yu, P.K., 2002. Corresponding dose response of radiographic film with layered gafchromic film. Phys.Med. Biol. 47, 285−289.

Capala, J., Stenstam, B., Skld, K., Munck af Rosenschld, P., Giusti, V., Persson, C., Wallin, E., Brun, A., Franzen, L., Carlsson, J., Salford, L., Ceberg, C., Persson, B., Pellettieri, L., Henriksson, R., 2003. Boron neutron capture therapy for glioblastoma multiforme: clinical studies in Sweden. J. Neurooncol. 62, 135−144.

Carlsson, J., et al., 2002. Radiation therapy through activation of stable nuclides. Acta Oncol. 41, 629−634.

Carrier, J.F., Archambault, L., Beaulieu, L., 2004. Validation of Geant4, an object-oriented Monte Carlo toolkit, for simulations in medical physics. Med. Phys. 31, 484−492.

Chadha, M., Capala, J., Coderre, J.A., Elowitz, E.H., Iwai, J., Joel, D.D., Liu, H.B., Wielopolski, L., Chanana, A.D., 1998. Boron neutron-capture therapy (BNCT) for glioblastoma multiforme (GBM) using the epithermal neutron beam at the Brookhaven National Laboratory. Int. J. Radiat. Oncol. Biol. Phys. 40, 829−834.

Coderre, J.A., Morris, G.M., 1999. The radiation biology of Boron Neutron Capture therapy. Radiat. Res. 151, 1−18.

De Stasio, G., Casalbore, P., Pallini, R., Gilbert, B., Sanita, F., Ciotti, M.T., Rosi, G., Festinesi, A., Larocca, L.M., Rinelli, A., Perret, D., Mogk, D.W., Perfetti, P., Mehta, M.P., Mercanti, D., 2001. Gadolinium in human glioblastoma cells for gadolinium neutron capture therapy. Cancer Res. 61, 4272−4277.

De Stasio, G., Rajesh, D., Casalbore, P., Daniels, M.J., Erhardt, R.J., Frazer, B.H., Wiese, L.M., Richter, K.L., Sonderegger, B.R., Gilbert, B., Schaub, S., Cannara, R.J., Crawford, J.F., Gilles, M.K., Tyliszczak, T., Fowler, J.F., Larocca, L.M., Howard, S.P., Mercanti, D., Mehta, M.P., Pallini, R., 2005. Are gadolinium contrast agents suitable for gadolinium neutron capture therapy? Neurol. Res. 27, 387−398.

Enger, S.A., Rezaei, A., Munck af Rosenschld, P., Lundqvist H, 2006a. Gadolinium neutron capture brachytherapy (GdNCB), a new treatment method for intravascular brachytherapy. Med. Phys. 33, 46−51.

Enger, S.A., Munck af Rosenschld, P., Rezaei, A., Lundqvist, H., 2006b. Monte Carlo calculations of thermal neutron capture in gadolinium: a comparison of GEANT4 and MCNP with measurements. Med. Phys. 33, 337−341.

Fortin, M.A., Petoral, R.M., Soderlind, F., Klasson, A., Engstrom, M., Veres, T., Kall, P.O., Uvdal, K., 2007. Polyethylene glycol-covered ultra-small Gd_2O_3 nanoparticles for positive contrast at 1.5 T magnetic resonance clinical scanning. Nanotechnology 18, 395501.

Franken, N.A.P., Bergs, J.W.J., Kok, T.T., Kuperus, R.R.N., Stecher-Rasmussen, F., Haveman, J., Van Bree, C., Stalpers, L.J.A., 2006. Gadolinium enhances the sensitivity of SW-1573 cells for thermal neutron irradiation. Oncol. Rep. 15, 715−720.

Gierga, D.P., Yanch, J.C., Shefer, R.E., 2000. An investigation of the feasibility for neutron capture synovectomy. Med. Phys. 27, 1685−1692.

Giusti, V., Munck af Rosenschold, P., Sköld, K., Montagnini, B., Capala, J., 2003. Monte Carlo model of the Studsvik BNCT clinical beam: description and validation. Med. Phys. 30, 3107−3117.

Goldenberg, D.M., Sharkey, R.M., Primus, F.J., Mizusawa, E., Hawthorne, M.F., 1984. Neutron-capture therapy of human cancer: In vivo results on tumor localization of boron-10-labeled antibodies to carcinoembryonic antigen in the GW-39 tumor model system. Proc. Nail. Acad. Sci. 81, 560−563.

Gonzalez, R.C., Woods, R.E., 2002. Digital Imaging Processing, pp. 189−191.

Goorley, T., Nikjoo, H., 2002. A comparison of three gadolinium based Approaches to cancer therapy. Radiat. Res. 154, 556−563.

Goorley, T., Kiger, W.S., Zamenhof, R.G., 2002. Reference dosimetry calculations for neutron capture therapy with comparison of analytical and voxel models. Med. Phys. 29, 145−156.

Harling, O.K., Riley, K.J., 2003. Fission reactor neutron sources for neutron capture therapy e a critical review. J. Neurooncol. 62, 7−17.

Hartman, T., Carlsson, J., 1994. Radiation dose heterogeneity in receptor and antigen mediated boron neutron capture therapy. Rad. Oncol. 31, 61−75.

Hawthorne, M.F., 1993. The role of chemistry in the development of boron neutron capture therapy of cancer. Angew. Chem. Int. Ed. Engl. 32, 950−984.

Hofmann, B., Fischer, C.O., Lawaczeck, R., Platzek, J., Semmler, W., 1999. Gadolinium neutron capture therapy (GdNCT) of melanoma cells and solid tumors with the magnetic resonance imaging contrast agent Gadobutrol. Invest. Radio. 34,126−133.

Hosmane, N.S., 2011. Boron Science: New Technologies and Applications. Taylor & Francis Books/CRC Press, Boca Raton, FL, USA.

Hosmane, N.S., Maguire, J.A., Zhu, Y., Takagaki, M., 2012. Boron and Gadolinium Neutron Capture Therapy for Cancer Treatment. World Scientific Pub., Singapore.

Jono, K., Ichikawa, H., Fujioka, K., Fukumori, Y., Akine, Y., Tokuuye, K., 1999. Preparation of lecithin microcapsules by a dilution method using the Wurster process for intraarterial administration in gadolinium neutron capture therapy. Chem. Pharm. Bull. 47, 54−63.

Kueffer, P.J., Maitz, C.A., Khan, A.A., Schuster, S.A., Shlyakhtina, N.I., Jalisatgi, S.S., Brockman, J.D., Nigg1, D.W., Hawthorne, M.F., 2013. Boron neutron capture therapy demonstrated in mice bearing EMT6 tumors following selective delivery of boron by rationally designed liposomes. Proc. Natl. Acad. Sci. 16, 6512−6517.

Le, U.M., Cui, Z., 2006a. Long-circulating gadolinium-encapsulated liposomes for potential application in tumor neutron capture therapy. Int. J. Pharm. 312, 105−112.

Le, U.M., Cui, Z., 2006b. Biodistribution and tumor-accumulation of gadolinium (Gd) encapsulated in long-circulating liposomes in tumor-bearing mice for potential neutron capture therapy. Int. J. Pharm. 320, 96−103.

Locher, G.L., 1936. Biological effects and therapeutic possibilities of neutrons. Am. J. Roentgenol. 36, 1−13.

Martin, R.F., DCunha, G., Pardee, M., Allen, B.J., 1988. Induction of double strand breaks following neutron capture by DNA bound ^{157}Gd. Int. J. Radiat. Biol. 54, 205−208.

Martin, R.F., DCunha, G., Pardee, M., Allen, B.J., 1989. Induction of DNA double-strand breaks by ^{157}Gd neutron capture. Pigment Cell Res. 2, 330−332.

Masiakowski, J.T., Horton, J.L., Peters, L.J., 1992. Gadolinium neutron capture therapy for brain tumors: a computer study. Med. Phys. 19, 1277e1284.

Matsumoto, T., 1991. Transport calculations of depth-dose distributions for gadolinium neutron capture therapy. Phys. Med. Biol. 37, 155e162.

Munck af Rosenschold, P., Ceberg, C.P., Giusti, V., Andreo P, 2002. Photon quality correction factors for ionization chambers in an epithermal neutron beam. Phys. Med. Biol. 47, 2397−2409.

Munck af Rosenschold, P., Giusti, V., Ceberg, C.P., Capala, J., Sköld, K., Persson, B.R., 2003. Reference dosimetry at the neutron capture therapy facility at Studsvik. Med. Phys. 30, 1569−1579.

Oyewumi, M.O., Mumper, R.J., 2003. Influence of formulation parameters on gadolinium entrapment and tumor cell uptake using folate-coated nanoparticles. Int. J. Pharm. 251, 85−97.

Poon, E., Verhaegen, F., 2005. Photon and electron physics in GEANT4. Med. Phys. 32, 1696−1711.

Salt, C., Lennox, A.J., Takagaki, M., Maguire, J.A., Hosmane, N.S., 2004. Boron and gadolinium neutron capture therapy. Russ. Chem. B+ 53, 1871−1888.

Shelly, K., Feakes, D.A., Hawthorne, M.F., Schmidt, P.G., Krisch, T.A., Bauer, W.F., 1992. Model studies directed toward the boron neutron-capture therapy of cancer: boron delivery to murine tumors with liposomes. Proc. Natl. Acad. Sci. 89, 9039−9043.

Shih, J.A., Brugger, R.M., 1992a. Gadolinium as a neutron capture therapy agent. Med. Phys. 19, 733−744.

Shih, J.A., Brugger, R.M., 1992b. Neutron induced brachytherapy: neutron capture therapy and Brachytherapy. Med. Phys. 19, 369−375.

Shikata, F., Tokumitsu, H., Ichikawa, H., Fukumori, Y., 2002. In vitro cellular accumulation of gadolinium incorporated into chitosan nanoparticles designed for neutron-capture therapy of cancer. Eur. J. Pharm. Biopharm. 53, 57−63.

Stepanek, J., 2003. Emission spectra of gadolinium-158. Med. Phys. 30, 41−43.

Sweet, W.H., 1997. Early history of development of boron neutron capture therapy of tumors. J. Neurooncol. 33, 19−26.

Takagaki, M., Hosmane, N.S., 2007. Gadolinium neutron capture. Aino J. 6, 39−44.

Tokumitsu, H., Ichikawa, H., Fukumori, Y., Block, L.H., 1999. Preparation of gadopentetic acid-loaded chitosan microparticles for gadolinium neutron-capture therapy of cancer by a novel Emulsion-Droplet coalescence technique.

Chem. Pharm. Bull. 47, 838−842.

Tokumitsu, H., Hiratsuka, J., Sakurai, Y., Kobayashi, T., Ichikawa, H., Fukumori, Y., 2000. Gadolinium neutron-capture therapy using novel gadopentetic acid-chitosan complex nanoparticles: in vivo growth suppression of experimental melanoma solid tumor. Cancer Lett. 150, 177−182.

Tokuuye, K., Tokita, N., Akine, Y., Nakayama, H., Sakurai, Y., Kobayashi, T., Kanda, K., 2000. Comparison of radiation effects of gadolinium and boron neutron capture reactions. Strahlenther Onkol. 176, 81−83.

Watanabe, T., Ichikawa, H., Fukumori, Y., 2002. Tumor accumulation of gadolinium in lipid-nanoparticles intravenously injected for neutron-capture therapy of cancer. Eur. J. Pharm. Biopharm. 54, 119−124.

X-5 Monte Carlo Team, 2003. MCNP - a General Monte Carlo N-particle Transport Code, Version 5, LA-UR-03−1987. Los Alamos National laboratory.